Separation Science and Technology
Publication details, including instructions for authors and subscription information:
http://www.informaworld.com/smpp/title~content=t713708471

Temperature-Swing Gas Separation with Electrothermal Desorption Step

M. Petkovska[a]; D. Tondeur[b]; G. Grevillot[b]; J. Granger[b]; M. Mitrović[c]
[a] FACULTY OF TECHNOLOGY AND METALLURGY, BELGRADE UNIVERSITY, BELGRADE, YUGOSLAVIA [b] CHEMICAL ENGINEERING LABORATORY CNRS-ENSIC NANCY, FRANCE [c] FACULTY OF TECHNOLOGY AND METALLURGY BELGRADE, UNIVERSITY BELGRADE, YUGOSLAVIA

To cite this Article Petkovska, M. , Tondeur, D. , Grevillot, G. , Granger, J. and Mitrović, M.(1991) 'Temperature-Swing Gas Separation with Electrothermal Desorption Step', Separation Science and Technology, 26: 3, 425 — 444
To link to this Article: DOI: 10.1080/01496399108050482
URL: http://dx.doi.org/10.1080/01496399108050482

SEPARATION SCIENCE AND TECHNOLOGY, 26(3), pp. 425–444, 1991

Temperature-Swing Gas Separation with Electrothermal Desorption Step

M. PETKOVSKA*
FACULTY OF TECHNOLOGY AND METALLURGY
BELGRADE UNIVERSITY
BELGRADE, YUGOSLAVIA

D. TONDEUR, G. GREVILLOT, and J. GRANGER
CHEMICAL ENGINEERING LABORATORY
CNRS-ENSIC
NANCY, FRANCE

M. MITROVIĆ
FACULTY OF TECHNOLOGY AND METALLURGY
BELGRADE UNIVERSITY
BELGRADE, YUGOSLAVIA

Abstract

Results of an experimental investigation of a new method for heating adsorbent beds in the desorption step owing to Joule's heat generated inside the adsorbent particles by passing an electric current through them are presented. Desorption of a previously saturated bed and cyclic separation with the electric potential applied to a fibrous activated carbon bed was performed.

INTRODUCTION

There are two conventional ways used to bring heat for thermal regeneration to saturated adsorbent beds: heating the bed through heat transfer surfaces and by the flow of a hot fluid. We attempted to use a third way: generating heat inside the adsorbent particles by passing an electric current through them. We give the name "electrothermal desorption" to this method which is presented in this article.

It should be pointed out that the phenomenon presented here is different from electroadsorption (*1*, *2*). In electroadsorption the thermodynamic

*To whom correspondence should be addressed.

property affecting the adsorption equilibrium is electric potential or electric charge, while in the electrothermal process it is the adsorbent temperature reached by electric heating.

Our investigation was based on the assumption that electrothermal desorption should have some advantages over conventional methods for the following reasons:

1) From a technological point of view, the direct electric energy supply could be simpler and easier to apply and control than indirect heating. Also, much larger heating rates can be applied.

2) From an energy point of view, electrothermal desorption could be more efficient.

3) From the aspect of desorption kinetics and dynamics, the same directions of the mass and heat fluxes—from the particle center to the surface and from the particles to the fluid (opposite to the direction of the heat transfer in the conventional methods of heating)—should make the electrothermal desorption superior because of thermal diffusion (*3*) and surface diffusion (*4*) effects.

4) From a design point of view, direct electric heating should enable different design solutions and the use of smaller equipment.

A very complex and extensive theoretical and experimental analysis would be necessary to prove all these statements. Nevertheless, the results of a rather simple experimental investigation of the problem, as presented in this work, prove some of them.

The experimental investigation included two parts: desorption experiments and cyclic temperature-swing experiments.

EXPERIMENTAL SYSTEM AND SET-UP

The adsorbent chosen for investigation of electrothermal desorption was fibrous activated carbon charcoal cloth (Ceca-Atochem, France). The adsorbent to be used has to be an electric conductor or semiconductor, so activated carbon is a convenient material. Fibrous activated carbon was chosen because of its handling properties and its excellent dynamic characteristics, which have often been mentioned in the literature (*5*, *6*). In addition, charcoal cloth has been recommended for use as an electric heater (*7*), which led us to the conclusion that it would be convenient for our investigation.

An organic vapor, 111-trichloroethane (T_{111}), was used as the adsorbate, and nitrogen was the carrier gas. The experiments were performed with the Atochem industrial T_{111} product with about 92% trichloroethane (density 1.3 g/cm^3).

The adsorbent bed was made of 20 layers of the activated carbon cloth, tightly pressed between two porous steel plates serving as electrodes and closed in a Teflon adsorption cell. The mass of the adsorbent bed was about 6 g, the diameter was 5 cm, and the thickness was 0.6 cm. The construction of the adsorption cell is shown in Fig. 1.

The fibrous activated carbon bed was connected to a closed electric circuit with a constant overall direct electric potential source. A small electrical resistance R_a (of about 0.1 Ω) was included in the circuit in series with the carbon bed, and connected to a recorder which served as an ammeter for measuring the current intensity I in the circuit. The electric potential drop across the bed, U_b, was also recorded. In this way it was possible to follow the electric resistance and the electric power transferred to the bed.

A constant gas flow rate was obtained by using a Brooks mass flow controller 5850 TR. The temperatures of the inlet and outlet gas, T_{gi} and T_{go}, and of the bed, T_b, were measured by using three chromel-alumel thermocouples and were registrated (an electronic device was used for switching the measuring point each 10 s).

For outlet gas concentration measurements a sampling cell of 100 cm^3 was used, and samples of 0.3 cm^3 were analyzed by capillary gas chromatography (a Delsi DI 700 instrument was used). A heat exchanger (a copper tube 0.5 m long of 0.6 cm o.d.) was inserted between the adsorption and the sampling cell in order to cool the outlet gas and to enable the gas samples to be taken at room temperature.

A schematic diagram of the experimental set-up is shown in Fig. 2.

DESORPTION EXPERIMENTS

In these experiments, desorption of the previously adsorbed T_{111} was performed by direct electrical heating of the adsorbent bed.

The adsorption step was performed in a closed system in which the adsorption cell was connected to a reservoir of known volume V_r and a pump (Fig. 2). A sample of liquid T_{111} (V_l = 1.5 cm^3) was injected into the reservoir, vaporized, and the gas mixture passed through the adsorption cell due to operation of the pump. After about half an hour, the time needed to reach equilibrium, the gas sample was taken from the reservoir and analyzed by gas chromatography. From the known quantity of injected T_{111}, $d_l V_l$, and the measured concentration in the gas phase at the end of the adsorption step C_0, the quantity of T_{111} adsorbed was calculated by using the mass balance

$$m_{ads} = d_l V_l - V_r C_0 \tag{1}$$

After turning the pump off and switching the three-way Valves V1 and

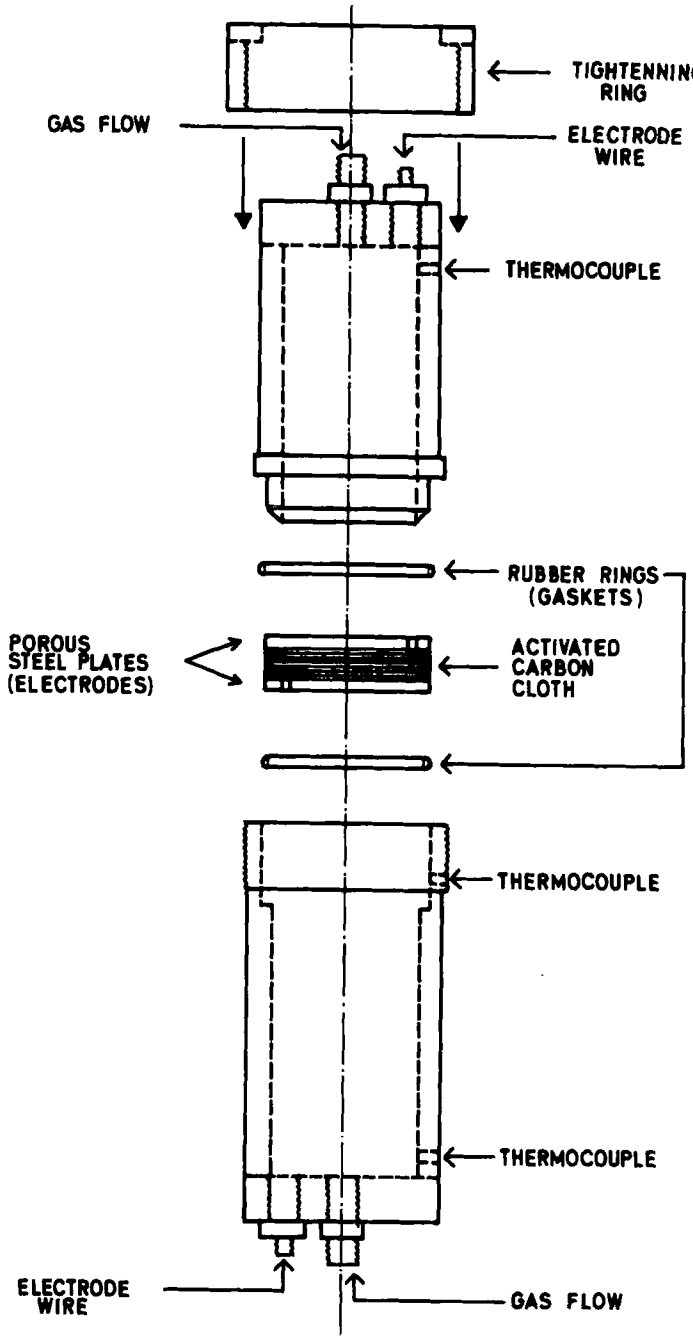

FIG. 1. Construction of the adsorption cell.

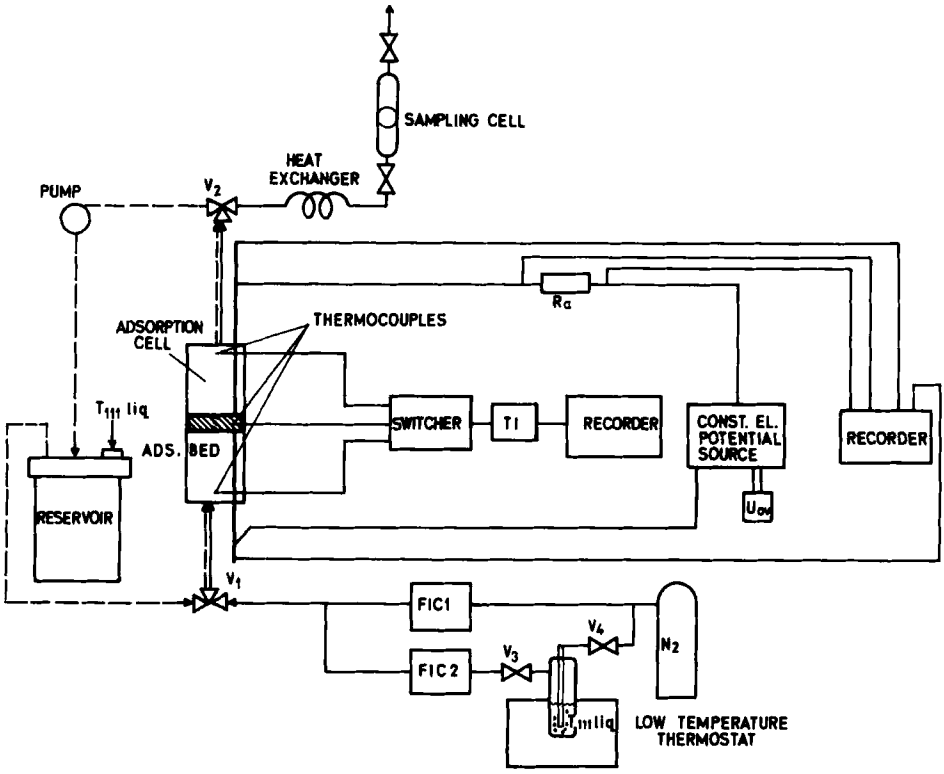

FIG. 2. Schematic diagram of the experimental set-up. (——) Gas flow during the desorption step of the desorption experiments and during the cyclic TSA experiments. (- - -) Gas flow during the adsorption step of the desorption experiments.

V2 (Fig. 2), the desorption step was started by simultaneously starting the pure nitrogen flow (Valves V3 and V4 closed) and closing the electrical circuit in which a constant overall electrical potential U_{ov} was imposed. The experiments were performed in the following range of parameters: overall electric potential, 3.5 to 5.4 V; gas flow rate, 2 to 6 dm^3/min. The upper limit of the electric potential and the duration of the experiments were chosen in order to keep the bed temperature lower than 200°C, in order to prevent damage of the Teflon cell.

The desorption curves (the outlet gas concentration changes during the desorption step) are shown in Fig. 3. The corresponding outlet gas (T_{go}) and bed temperatures (T_b) are presented in Fig. 4. The inlet gas temperature T_{gi} was practically constant—about 22°C.

The changes of the electric resistance with time are presented in Fig. 5 and the power supplies in Fig. 6.

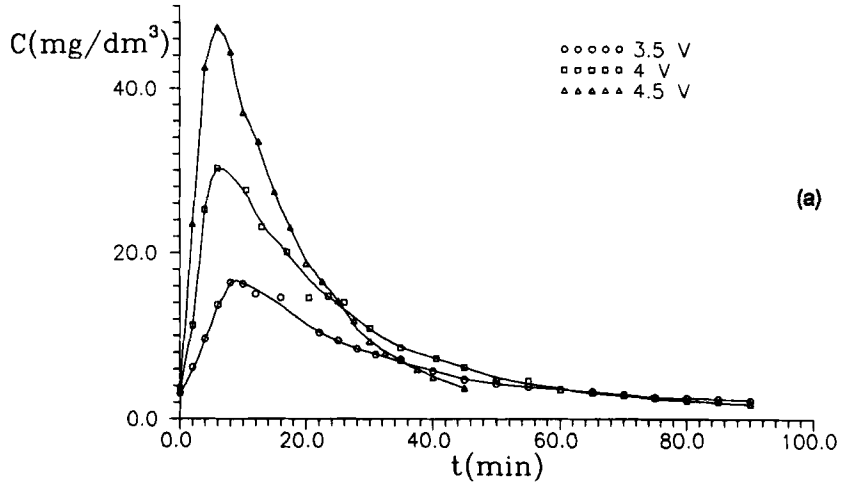

FIG. 3. Desorption curves obtained for different flow rates: (a) 2 dm³/min, (b) 4 dm³/min, (c) 6 dm³/min.

The electric resistance of the bed was calculated as the ratio of the measured electric potential drop across the adsorbent bed and the electric current intensity in the circuit:

$$R_b = U_b/I \tag{2}$$

and the electric power supply as their product:

$$P_b = U_b I \tag{3}$$

Reviews of the desorption experiments are given in Tables 1 and 2. For each experiment, defined by the overall electric potential applied U_{ov} (V) the gas flow rate $\dot{V}$(dm³/min), and the duration of the experiment τ (min), the values of the maximal outlet gas concentration C_{max} (mg/dm³), the average outlet gas concentration during the first 10 min of the desorption step $\langle C\rangle_{10}$ and during the entire experiment $\langle C\rangle_{tot}$, and the percentage of the quantity desorbed to the previously adsorbed quantity of T_{111} during the first 10 min. D_{10} (%) and during the whole experiment D_{tot} (%), are given in Table 1.

In Table 2 the quantities related to the thermal behavior of the system are reviewed: the final bed and outlet gas temperatures T_{bf} and T_{gof}, the average bed and outlet gas temperatures $\langle T_b\rangle$ and $\langle T_{go}\rangle$, the rate of the

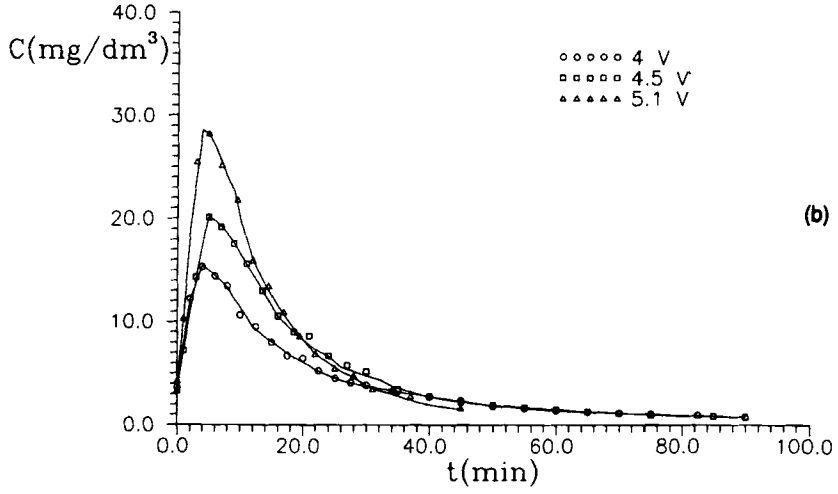

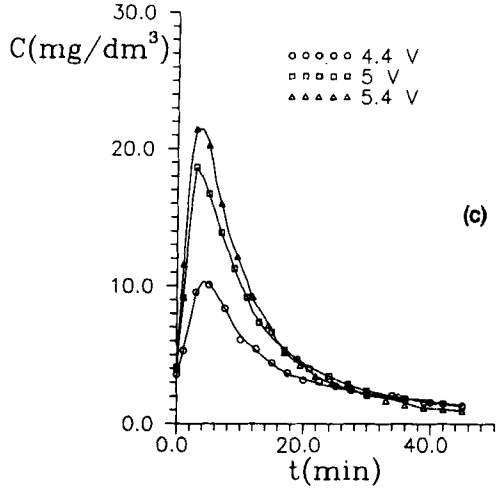

bed temperature change at the beginning of the experiment $(dT_b/dt)_0$, the average power supply $\langle P \rangle$, and the ratios

$$W = \frac{T_{gof} - T_{gi}}{T_{sf} - T_{gi}} \tag{4}$$

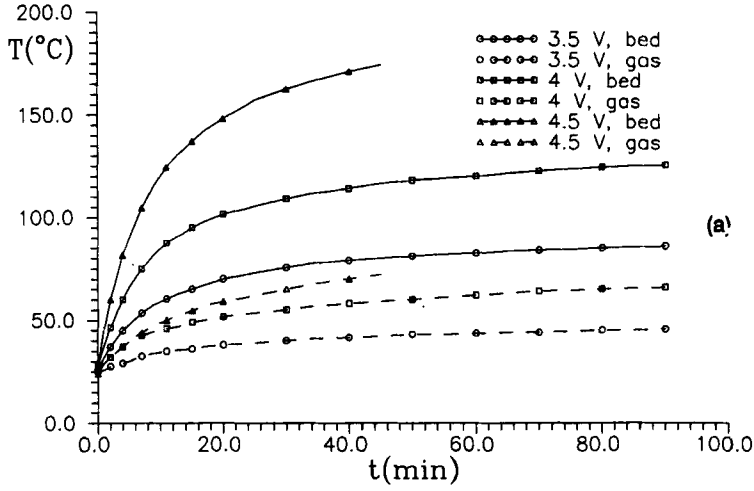

FIG. 4. Bed and outlet gas temperatures during the desorption experiments for different flow rates: (a) 2 dm³/min, (b) 4 dm³/min, (c) 6 dm³/min.

and

$$Z = \frac{V d_g c_{pg} (T_{gof} - T_{gi})}{P_f} \tag{5}$$

which will be explained later in the text.

According to Fig. 4, the bed and the outlet gas temperatures increase with time and reach some stationary state after about 60 min. For one flow rate, higher temperatures are obtained with higher potentials (corresponding to higher energy consumption), and for one electric potential the temperatures are lower for higher flow rates (corresponding to higher energy removal by gas convention).

It should be pointed out that in each experiment the outlet gas reaches much lower temperatures than the adsorbent bed. The adsorption equilibrium is governed by the temperature of the solid and not of the fluid phase. Contrary to conventional thermal desorption techniques, the electrothermal method enables the adsorbent particles to be heated to the needed desorption temperature with the gas heated to some considerably lower temperature. For large systems, this could give considerable energy savings.

The quantity W, defined by Eq. (4) and given in Table 2, represents the ratio of the energy spent for heating the gas in electrothermal desorption and the energy that should be spent for the same purpose in conventional

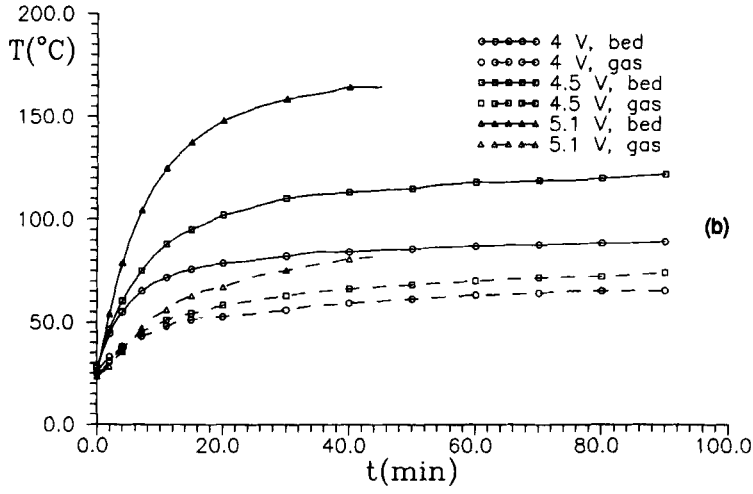

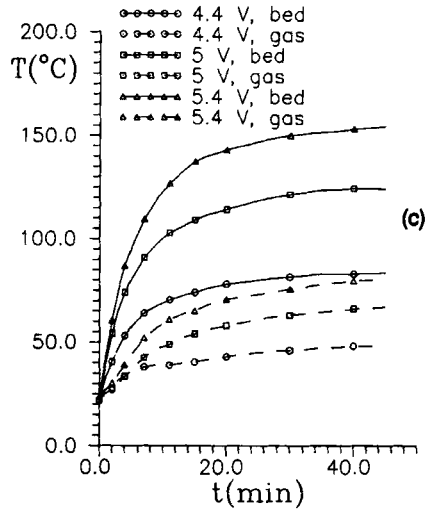

methods (where the gas has to be heated to the desorption temperature). The reciprocal value, $1/W$, gives some data about the effectiveness of our method compared to conventional methods. It can be seen from Table 2 that W is low (in most cases less than 0.5) and increases to some extent with increasing flow rate. Notice that W is lower for experiments lasting 45 min because in these cases a stationary state is not reached.

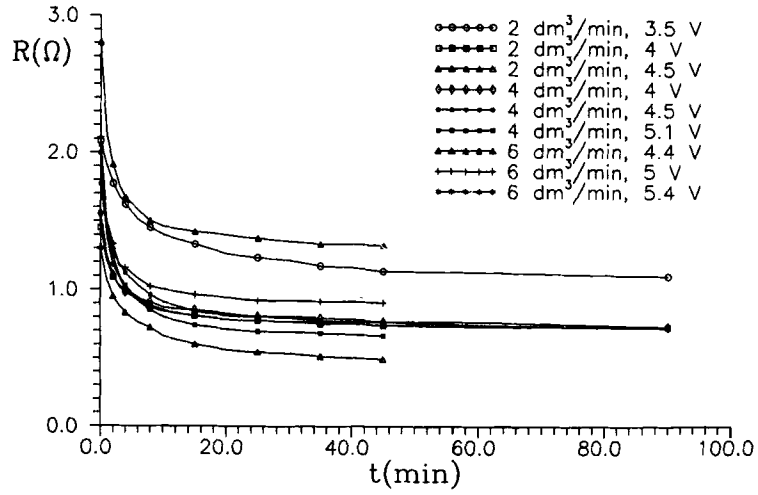

FIG. 5. Electric resistance of the adsorbent bed during the desorption experiments.

The adsorption cell was not insulated, so heat losses were substantial. The thermal efficiency parameter Z, defined by Eq. (5) is the ratio of the energy transferred to the gas and the total energy given to the bed at the end of each experiment when the stationary state was achieved or nearly achieved and desorption was practically finished. It could be considered

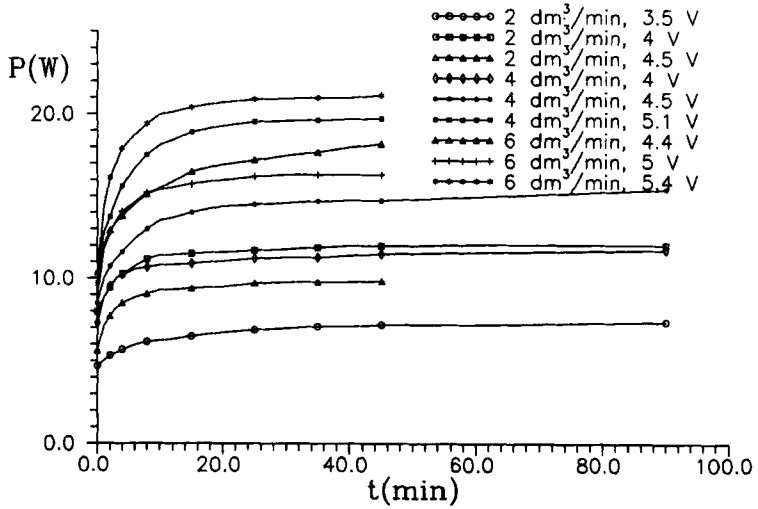

FIG. 6. Electric power transferred to the adsorbent bed during the desorption experiments.

TABLE 1
Review of the Desorption Experiments—Part I

Experiment	$\dot{V}$	U_{ov}	τ	C_{max}	$\langle C\rangle_{10}$	$\langle C\rangle_{tot}$	D_{10}	D_{tot}
1	2	3.5	90	16.7	10.9	6.5	11.2	60.2
2	2	4	90	30.2	22.0	8.6	22.7	87.5
3	2	4.5	45	47.4	38.5	19.9	39.9	92.8
4	4	4	90	15.6	12.3	3.9	25.4	73.1
5	4	4.5	90	20.2	15.4	4.9	31.9	90.4
6	4	5.1	45	30.8	23.7	10.4	46.3	91.7
7	6	4.4	45	11.9	8.1	4.0	25.2	55.6
8	6	5	45	18.7	13.8	5.8	43.0	81.7
9	6	5.4	45	21.4	16.1	6.2	49.1	87.3

that all the energy not transferred to the gas was lost. The values of Z given in Table 2 are low, which shows that the heat losses were very high. These high heat losses contribute to the slow dynamics of the thermal behavior of the system. For real applications, adiabatic conditions should be obtained.

The electric resistance of the bed decreases with time, reaching some stationary value after some time (Fig. 5). The resistance decrease is the result of the adsorbent temperature increase. This semiconductor behavior of the fibrous activated carbon was expected (*5*, *6*).

As a result of the resistance decrease, the electric power transferred to the bed (defined by Eq. 3) increases with temperature rise, i.e., with time (Fig. 6).

For the same gas flow rate, the electric resistance is lower and the power supply is higher for any higher electric potential applied, but for one value

TABLE 2
Review of the Desorption Experiments—Part II

Experiment	T_{sf}	T_{gof}	$\langle T_s\rangle$	$\langle T_{go}\rangle$	$(dT_s/dt)_0$	$\langle P\rangle$	W	Z
1	86	45.5	75	40	5	7.0	0.37	0.12
2	126	66	104	56	8	11.7	0.42	0.14
3	174	71.5	140	56	16.5	16.5	0.33	0.11
4	88	65	81	57	8	11.3	0.65	0.29
5	122	74	107	63	12.5	14.3	0.52	0.27
6	163	82	136	64	17.5	18.5	0.43	0.24
7	83.5	48	74	41	11	9.4	0.42	0.31
8	125	67	99	55	15	15.6	0.44	0.32
9	154.5	80	130	66	20	20.1	0.44	0.32

of electric potential the electric resistance is somewhat higher and the power supply is somewhat lower for a higher gas flow rate, corresponding to lower temperatures.

From Fig. 3 and Table 1 it can be seen that the maximum of the desorption curve occurs quickly and is followed by a tailing desorption wave. For one value of the gas flow rate the outlet gas concentration and the percentage desorbed are higher for higher electric potential, corresponding to higher temperatures reached and higher energy consumption (Figs. 4 and 6, Table 2). For the same value of the electric potential (Cases 2 and 4 and Cases 3 and 5), higher concentrations and higher percentage desorbed were obtained for a lower flow rate, corresponding to higher temperatures (according to lower energy removal from the adsorbent bed by gas convection) and to somewhat higher power supplies.

An attempt was made to obtain the same bed temperatures with different combinations of gas flow rates and electric potentials. To some extent this was achieved in Cases 2 and 5. In these two experiments a higher outlet gas concentration was obtained with a lower flow rate and electric potential (Case 2), but the percentage desorbed was higher for a higher flow rate and electric potential (Case 5).

According to the desorption results presented, we conclude that the desorption rate depends mostly on the temperature of the bed and on the rate of the bed temperature rise at the beginning of the experiment. The slow dynamics of thermal behavior is thus inconvenient.

An attempt was made to reach the wanted temperature in a short period of time by applying a relatively high initial electric potential and then lowering the electric potential in order to keep the temperature constant. The desorption curve obtained in this way with a gas flow rate of 2 dm^3/min and an electric potential of 7 V during the first 1.7 min and 4 V later is presented in Fig. 7(a). The corresponding bed temperature is given in Fig. 7(b). The bed temperature was about 120°C and the outlet gas concentration at the beginning was quite high (the detected peak concentration is 100.66 mg/dm^3, and the real one was probably much higher). This method seems very convenient, but it requires continuous concentration measurement which was not available for our experiments.

It should be pointed out that in the system with a constant overall potential in the circuit, none of the electric quantities related to the adsorbent bed (R_b, P_b, I, U_b) is constant because the resistance of the bed, and therefore the total resistance in the circuit, decreases with time.

Because the energy supply changes while the bed is being heated, a system with constant electric potential is not easy to control. We think that a system with a constant energy supply would be much more convenient.

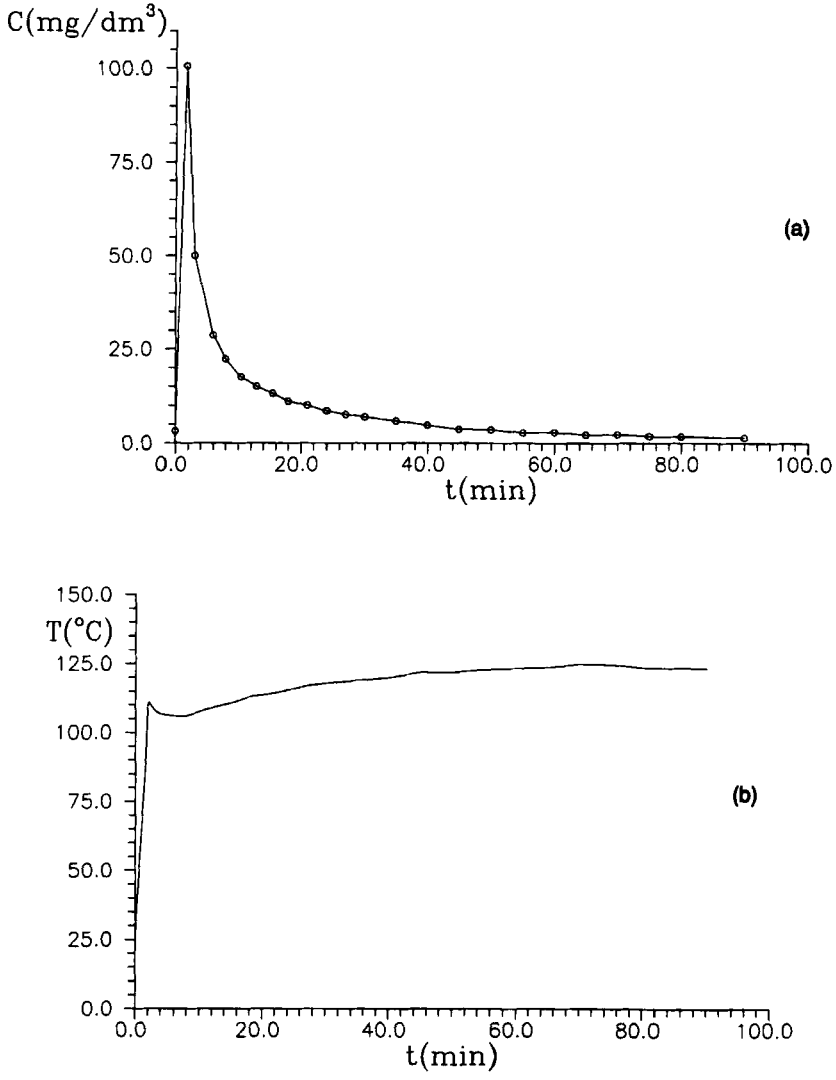

FIG. 7. Desorption with variable electric potential supply: $U_{ov1} = 7$ V, $U_{ov2} = 4$ V, $\dot{V} = 2$ dm³/min. (a) Outlet gas concentration, (b) bed temperature.

CYCLIC TEMPERATURE-SWING EXPERIMENTS

Separation of the T_{111} vapor and nitrogen was performed by cycling the overall electric potential in the circuit between zero and some constant value (in the form of square waves).

Although our study was performed as a potential-swing experiment, we consider this process to be a temperature-swing experiment because the thermodynamic property governing the adsorption equilibria is the adsorbent bed temperature.

A continuous feed stream with about 15 mg/dm^3 T_{111} in nitrogen was obtained by mixing two gas streams: one of pure nitrogen (~80% by volume) regulated by mass flow controller FIC1, and the other nearly saturated with T_{111} at −20°C (~20% by volume) regulated by the mass flow controller FIC2 (Valves V3 and V4 in Fig. 2 opened, and the positions of Valves V1 and V2 the same as during the desorption step of the desorption experiments). This mixture was fed to the adsorption cell, and the overall electric potential in the system was cycled. The outlet gas concentration, the gas and bed temperatures, the current intensity, and the electric potential drop across the adsorbent bed were measured.

Experiments with V = 2 and 4 dm^3/min were performed for a few values of the potential changes and of the cycling period. In each experiment the adsorbent bed was previously saturated by T_{111} in equilibrium with the feed stream, and the cycling was started at a high potential, i.e., the first half-cycle was hot.

A review of the temperature-swing results is given in Tables 3 and 4. For each experiment determined by the values of the gas flow rate $\dot{V}$, the overall electric potential during the hot half-cycle U_{ov}, the hot and cold cycle periods τ_h and τ_c, and the concentration of the feed stream C_0, Table 3 contains the average outlet gas concentration during the hot $\langle C\rangle_h$ and the cold $\langle C\rangle_c$ half-cycle and the separation factor defined as their ratio:

$$\alpha = \langle C\rangle_h/\langle C\rangle_c \tag{6}$$

In Table 4 the thermal and energy parameters are presented: the bed temperature at the end of the hot and of the cold half-cycle, T_{sh} and T_{sc}

TABLE 3
Review of the Temperature-Swing Experiments—Part I

Experiment	$\dot{V}$	U_{ov}	τ_h	τ_c	C_0	$\langle C\rangle_h$	$\langle C\rangle_c$	α
1	2	4	20	20	15.76	25.31	3.06	8.28
2	2	4	30	30	16.41	30.52	1.77	17.22
3	2	4.5	20	30	15.74	34.44	1.43	24.08
4	2	4.5	30	45	16.07	35.72	0.89	40.01
5	4	4.5	20	20	13.14	24.31	1.36	17.88
6	4	5.1	20	20	14.53	24.93	1.16	21.45
7	4	5.1	30	30	14.30	24.85	0.93	26.73

TABLE 4
Review of the Temperature-Swing Experiments—Part II

Experiment	T_{sh}	T_{sc}	$\langle T_s \rangle_h$	$\langle T_s \rangle_c$	$\langle P \rangle_h$	$\langle P \rangle_{tot}$
1	113	37	92	55	10.6	5.3
2	121	33.5	100	51	10.9	5.5
3	147	35	117	55	15.2	6.1
4	155.5	32.5	125	53	15.5	6.2
5	134.5	35	111	55	15.5	7.8
6	174	41	138	68	21.4	10.7
7	181	36	153	60	22.2	11.1

(the maximal and minimal temperature during one cycle); the average bed temperature during the hot and the cold half-cycle. $\langle T_s \rangle_h$ and $\langle T_s \rangle_c$; and the average electric power supply during the hot half-cycle $\langle P \rangle_h$ and during the whole cycle $\langle P \rangle_{tot}$. As the electric power during the cold half-cycle is zero:

$$\langle P \rangle_{tot} = \langle P \rangle_h \tau_h / (\tau_h + \tau_c) \tag{7}$$

One experiment that gave the smallest separation factor (Case 1) and another that gave the largest one (Case 4) are presented graphically in Figs. 8 and 9, respectively (the outlet gas concentration, the bed temperature, and the power transferred to the adsorbent bed are given).

It was noticed that the temperature and the power supply did not repeat in the first few cycles. This behavior was more significant in the experiments with shorter cold half-cycles and higher potentials applied. This phenomenon results from the fact that at the beginning of the cycle, the bed temperature was higher, and accordingly the electric resistance was lower than at the beginning of the previous cycle. In a system with constant electric potential, this results in a higher power supply and in higher temperatures reached.

These changes could be considered unimportant after the third cycle (a quasi-stationary state was nearly reached).

The values given in Tables 3 and 4 correspond to the third cycle of each experiment.

As expected, higher values of the separation factor were obtained with higher potentials (corresponding to higher temperatures during the hot half-cycle and higher energy consumption). For the same values of the gas flow rate and electric potential, better separation (higher separation factor and lower concentration during the cold half-cycle) was obtained for longer cycle times. Especially good results were obtained for asymmetric cycles

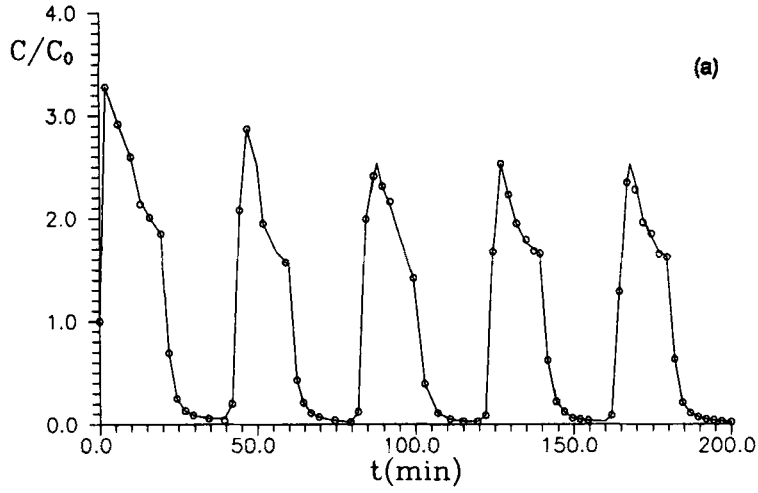

FIG. 8. TSA results for Case 1 (U_{ov} = 4 V, $\dot{V}$ = 2 dm³/min, τ_h = 20 min, τ_c = 20 min): (a) outlet gas concentration, (b) bed temperature, (c) electric power.

with a longer cold half-cycle (Cases 3 and 4): high separation factors correspond to low average power during one cycle, $\langle P \rangle_{tot}$.

The temperature decrease during the cold half-cycle was mainly the result of heat losses in the system. To some extent it was influenced by the gas flow rate, but, as the heat transfer between the solid and fluid phases was low, this influence was not great. Separation could be improved if faster cooling of the bed during the cold half-cycle was achieved.

The best results would be obtained if the hot half-cycle was adiabatic (which would result in a faster temperature rise and therefore higher effluent concentrations) and the bed was cooled during the cold half-cycle. Asymmetric cycles with short half-cycles with a high electric potential and a high power supply followed by longer cold half-cycles would be especially interesting.

DISCUSSION AND CONCLUSIONS

Although the results presented in this paper were obtained using a simple experimental system, they show that the idea of direct electric heating of an adsorbent bed is interesting and applicable. Desorption is rapid and mainly dependent on the temperature reached. The method is superior to conventional ones from the energy point of view.

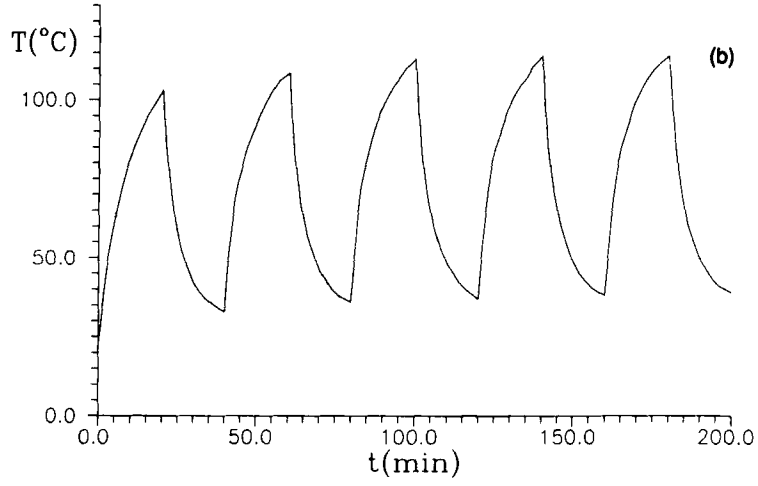

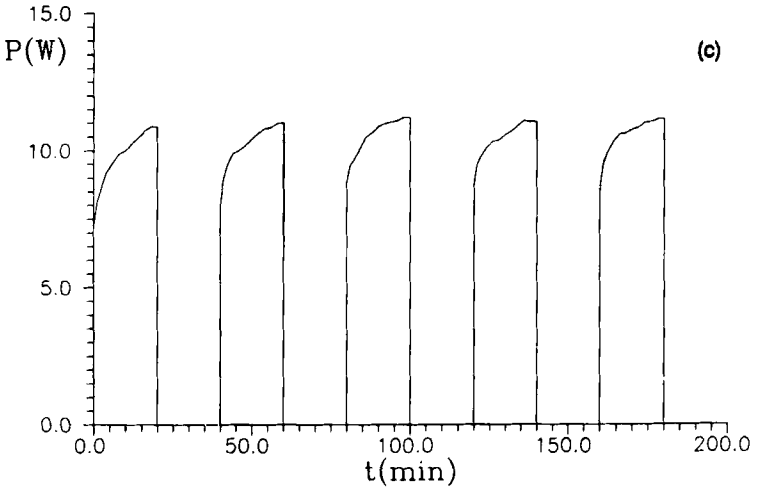

For adsorbents with temperature-dependent electric resistance (as in our case), a system with a constant power supply would be more convenient for control.

It should be pointed out that the temperature of the adsorbent bed is nonuniform in both the axial and radial directions. The measured bed temperature was regarded as a single representative value. The existence

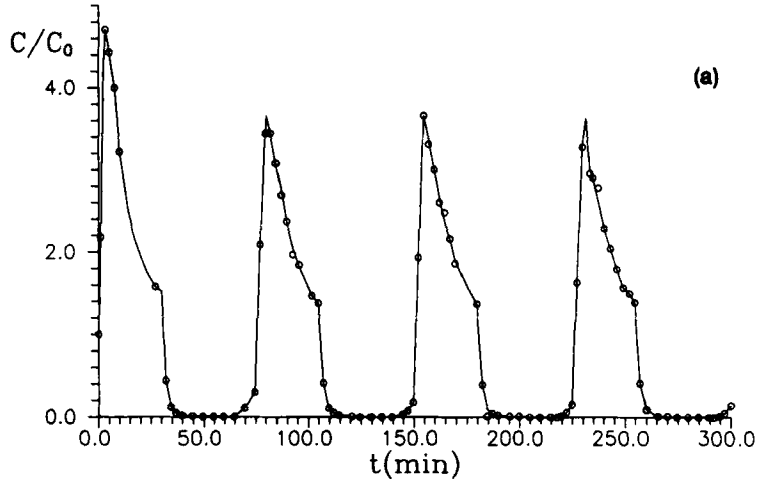

FIG. 9. TSA results for Case 4 (U_{ov} = 4.5 V, $\dot{V}$ = 2 dm³/min, τ_h = 30 min, τ_c = 45 min): (a) outlet gas concentration, (b) bed temperature, (c) electric power.

of hot spots in the bed is also possible (the electric contacts among the adsorbent fibers are different and not defined), so this method would not be convenient for the desorption of thermally unstable substances.

The proposed method could be broadly used for adsorbent regeneration, gas separation, and solvent regeneration. It would also be interesting to try the method on liquid–solid systems.

Further experimental investigations of electrothermal desorption should proceed in the following directions:

1) A search for the best adsorbent forms (carbon monofilament fibers, carbon fiber paper, integrated forms made of active charcoal) with stable electrical contacts, independent of the time and bed conditions.

2) Optimization of the lengths and shapes of potential changes in electrothermal TSA processes.

3) A search for the best design and technical solution of separation equipment (adsorption columns, porous wall tubes, rotating cylinders).

SYMBOLS

C concentration (mg/dm³)
c specific heat (J/g/°C)
D ratio of desorbed and previously adsorbed quantity (%)
d density (g/cm³)

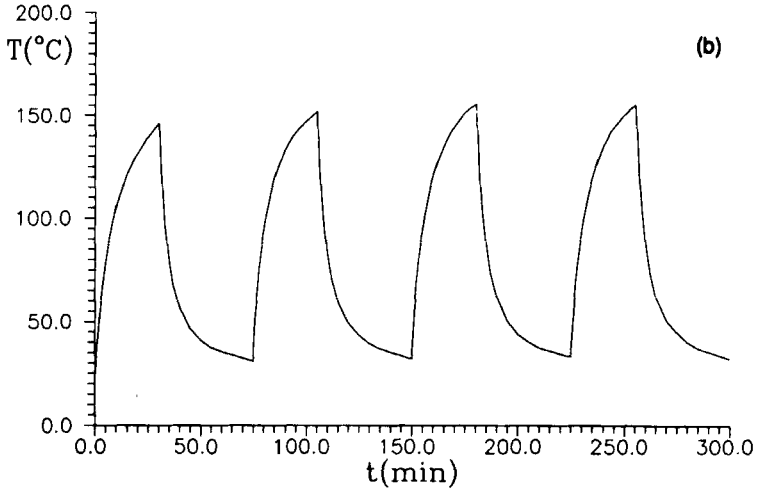

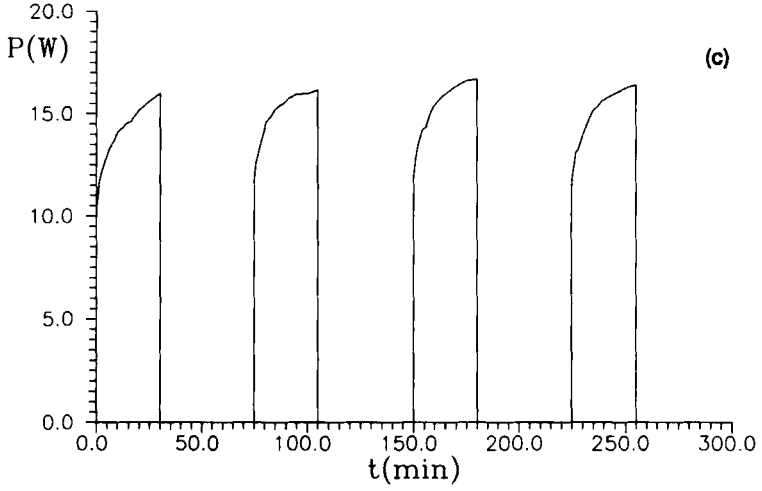

I	electric current intensity (A)
P	electric power (W)
R	electric resistance (Ω)
T	temperature (°C)
t	time (min)
U	electric potential (V)
V	volume (cm^3)

$\dot{V}$ volumetric flow rate (dm^3/min)
W nondimensional parameter defined by Eq. (4)
Z nondimensional parameter defined by Eq. (5)
$\langle\rangle$ time average value

Greek Symbols

τ experiment or cycle duration (min)
α separation factor (nondimensional)

Subscripts

0 initial, feed
g gas
b bed
f final
o outlet
i inlet
r reservoir
l liquid T_{111}
c cold
h hot
10 corresponding to the first 10 min
tot corresponding to the whole experiment or cycle time

REFERENCES

1. Y. Oren and A. Soffer, *J. Electrochem. Soc., 125,* 869 (1978).
2. J. H. Strohl and K. L. Dunlap, *Anal. Chem., 44,* 2166 (1972).
3. R. B. Bird, W. E. Stewart, and E. N. Lightfoot, *Transport Phenomena,* Wiley, New York, 1966.
4. P. C. Carman, *Flow of Gases through Porous Media,* Butterworths, London, 1956.
5. M. E. Smith and J. A. Davies, in *Proceedings of the 16th Biennial Conference on Carbon,* San Diego, California, 1983, p. 323.
6. H. Komagata, S. Ohmori, N. Ishizaki, and N. Shimada, in *Proceedings of the International Symposium on Carbon: New Processing and New Application,* Jouyhagashi, Japan, 1982, p. 549.
7. Charcoal Cloth, prospect material.
8. Group of French authors, *Les Carbones,* Vol. 1, Maison, Paris, 1965.
9. K. Sugihara, I. Rahim, M. Z. Tahar, and M. S. Dresselhaus, in *Proceedings of the 17th Biennial Conference on Carbon,* University of Kentucky, Lexington, Kentucky, 1985, p. 225.

Received by editor March 1, 1990